IEEE Access
Multidisciplinary ⋮ Rapid Review ⋮ Open Access Journal

Received 7 September 2023, accepted 13 September 2023, date of publication 18 September 2023,
date of current version 27 September 2023.

Digital Object Identifier 10.1109/ACCESS.2023.3316692

RESEARCH ARTICLE

Implementation of Rehabilitation Modalities Using a Low-Cost PAM Actuated Robotic Orthosis

CABBAR V. BAYSAL, (Senior Member, IEEE)
Department of Biomedical Engineering, Cukurova University, 01330 Adana, Turkey
e-mail: cvbaysal@cu.edu.tr

This work was supported in part by the Scientific Research Projects Coordination Unit of Cukurova University.

ABSTRACT Robotic rehabilitation is a solution for recovery from neuromuscular diseases and supports physical therapists in performing high-intensity and repetitive training activities. The main reason for the limitations of rehabilitation robot utilization is economic factors because rehabilitation robot technology requires high levels of investment and relatively costly routine operation and maintenance. To facilitate widespread adoption of rehabilitation robots, low-cost, highly compliant, and simple-to-operate robotic rehabilitation devices are required. In this study, to introduce a novel alternative solution to the aforementioned problem, a low-cost, highly transparent, single pneumatic artificial muscle (PAM) actuated robotic therapy orthosis that enables the patient to perform all training modalities is introduced. A novel control approach was developed by combining admittance control and inverse-dynamics-based compliant controls. By means of simple counterweight loads and compliant control, quasi-static movement of the orthosis for active exercises is achieved for the full operation range of PAM without any jerky transitions. A new assist-active modality named "Patient Activated Assistance" (PAAM) was introduced, in which the patient was the master, and the exercise was performed as long as the patient was active, avoiding slacking. Assistance was provided by sharing the load force in accordance with the applied gain. The orthosis performance in realizing the training modalities was verified using surface electromyogram (sEMG) measurements. The results demonstrated that the proposed low-cost single-PAM-actuated robotic orthosis could be a solution to robotic rehabilitation demands, especially in low-middle-income countries (LMIC).

INDEX TERMS Rehabilitation robotics, robotic orthosis, training modalities, pneumatic artificial muscle, compliant control.

I. INTRODUCTION

In recent years, neuromuscular diseases such as stroke and neural injuries have affected millions of people with disabilities worldwide. According to the fact sheet of the WSO for 2022, the global cost of stroke reaches %1.2 of GDP [1]. The main stroke burden in the world is in low-middle-income countries (LMIC). Rehabilitation is a key solution to recovery from neuromuscular diseases that utilizes different disciplines to improve the quality of life of people with disabilities caused by chronic diseases [2]. Rehabilitation involves motor recovery via neuronal plasticity through controlled, repetitive, and variable exercise patterns. The definitions of the rehabilitation phases and recovery timeline for post-stroke are provided in [3]. Especially for upper extremity disabilities, it is critically important to have rehabilitation in the early phases, such as the subacute and acute phases [4]. Clinical findings indicate that for many patients, the rehabilitation process should begin in hospital for many patients [2]. An understanding of the brain's recovery processes, called the computational motor learning perspective, shows that for many patients, a significant portion of behavioral improvement and rapid changes occur between the first weeks and months after a stroke. Therapeutic interventions during this period contributed significantly to recovery [5].

In rehabilitation, the duration and intensity of the therapy sessions are critical factors that affect recovery. Proper adjustment of therapy dosage, intensity, number of repetitions, and

The associate editor coordinating the review of this manuscript and approving it for publication was Yangmin Li.

This work is licensed under a Creative Commons Attribution-NonCommercial-NoDerivatives 4.0 License.
For more information, see https://creativecommons.org/licenses/by-nc-nd/4.0/

execution of task-oriented training enhances plasticity and functional recovery. To overcome the limitations of conventional therapy, robot-assisted rehabilitation approaches have been developed to support physical therapists in performing high-intensity and repetitive training activities, as a more effective and stable rehabilitation process. Moreover, robotic assistance helps reduce the physical burden on therapists, who can support multiple patients. During rehabilitation, robotic devices can increase afferent inputs from the peripheral joints and task-specific stimulation of the central nervous system, which enhances functional recovery according to the principles of neuroplasticity and motor learning [6].

Numerous reviews have assessed the efficacy of robotic rehabilitation [7], [8], [9], [10], [11], [12]. In these reviews, the performance of robotic rehabilitation systems was evaluated based on published clinical results, and similar opinions for robotic rehabilitation methods are effective, practical, and useful for therapies in collaboration with physical therapists have been expressed. Moreover, reviews have been conducted regarding the technological aspects of robotic rehabilitation devices. For instance, in [13], the authors provided an overview of existing robotic rehabilitation devices with classifications according to applications and usage, such as the upper and lower extremities. In addition, they concluded that, although there are many applied robots for neurorehabilitation, future studies should concentrate on the development of more compliant control algorithms with novel mechatronic structures that are lightweight, efficient, compliant, and portable. The review given in [14] focused on upper-extremity robotic rehabilitation devices and classified them according to aspects of the application field, type of assistance, mechanical design, control strategy, and clinical evaluation. The end-effector and exoskeleton devices are the main categories of robotic rehabilitation systems. An up-to-date review discussing recent advancements in upper-extremity rehabilitation robotics was presented in [15]. Although there are many comprehensive reviews covering lower-extremity robotic rehabilitation systems, such as [16] and [17], the main citations are made from upper-extremity systems because of their relevance to the work presented in this text.

One of the most important issues in rehabilitation robotics is the application of training modalities in therapy. The training modalities form the human-robot interaction format during rehabilitation to start the recovery process and induce motor plasticity. Training modalities for rehabilitation are mainly classified as ''passive,'' ''active-assisted,'' ''active'' and ''resistive.'' The training modalities are clearly illustrated in [18] as a review of the framework for the upper extremity, and robotic devices are classified according to the training modalities. In [19], the authors reviewed patient-cooperative control strategies for upper limb rehabilitation robots from a multidisciplinary perspective. Reviews of the control strategies and methods available for robotic devices are presented in [20] and [21]. According to these authors, the implementation of highly compliant control methods is crucial. The control strategies commonly used at high levels include impedance/admittance-based strategies, adaptive/intelligent control techniques, and physiological signal-based control. For compliant control, a basic review of the concepts and classification of the applied methods is provided in [22]. The authors in [23] presented a taxonomy of algorithms for compliant control and stated that in the case of human–robot interaction, compliant control is essential in unstructured environments because it controls energy transfer to the environment and forms a safe interaction. Impedance/admittance-based control strategies are widely used for high-level control of rehabilitation robots [24]. An overview of admittance control for human–robot interactions, considering stability and passivity, is given in [25]. Classical PD/PID is the most frequently used controller for low-level control of robotic systems. Many designers consider back-drivable mechanical structures; however, most robotic rehabilitation devices are not inherently transparent. Most of these utilize variable-stiffness actuators, sensors, and high-level control algorithms to improve patient cooperation in therapies, resulting in complicated and costly structures.

Although robotic rehabilitation devices have demonstrated efficacy, there are factors limiting their widespread adoption in clinics and homes. The primary reasons for the limitations of rehabilitation robot utilization are high economic costs, low user friendliness, and various clinical practice settings [26]. Among them, economic factors step forward because these robots are very expensive, and neither clinics nor patients can afford them, especially in LMIC, because rehabilitation robot technology requires high levels of investment and relatively costly routine operations and maintenance [27]. The development of cost-effective robotic rehabilitation devices that can work in rough environments under limited expert supervision and are produced at a low economic cost is the main solution to the rehabilitation processes in LMIC [28]. In general, exoskeleton robots are more complex than end-effector robots; hence, greater complexity results in a higher cost of technology. Many studies have demonstrated that end-effector robots are a low-cost solution for the treatment of upper limb proximal joints such as the shoulder and elbow. In addition, single-joint robotic training can yield significant results similar to multi-joint functional robotic training. Therefore, a robot with one degree of freedom (DOF) is still a reasonable option for rehabilitation compared to multi-DOF training [29]. Such a design approach could alleviate the complexity of the rehabilitation robot's design, making it more affordable by reducing the cost while increasing portability and usability. Robotic orthoses with compliant structures could be considered alternative solutions because they are affordable as low-cost therapeutic devices. A review criticizing current and emerging actuator technologies for compliant robotic orthoses was provided [30]. The results clearly indicate that high compliance could arise from either the actuator type or the applied control

method. Most robotic devices use motor-driven and geared solutions with variable stiffness actuators, which are costly. Alternatively, PAM actuators are inherently compliant and low-cost actuators with a high force-to-weight ratio and a flexible structure. Furthermore, the inherent compliance makes PAM feasible for rehabilitation robots. However, PAM has high nonlinearity, hysteresis, and time-varying characteristics, resulting in difficulties in modeling and control actions, which are limiting factors for its use. An up-to-date review of rehabilitation robots actuated by pneumatic artificial muscles was provided [31]. In this review, the authors analyzed the mechanical structures and control strategies of pneumatic muscle-actuated rehabilitation robots. Soft rehabilitation robots are classified and reviewed according to their actuation configuration. Another important aspect critically inspected was the advanced control strategies applied to different mechanical designs to overcome the highly nonlinear and time-varying characteristics of PAM. In addition, it was indicated that almost all the developed robots were not tested for the implementation of complete rehabilitation training modes, which forms a gap between the designs and clinical applications. Many existing studies have focused on the application of high-level control methods for accurate trajectory tracking rather than their therapeutic use [32]. For instance, in [33], an active knee rehabilitation robot actuated by antagonistic dual PAM was described, and it was modeled using the ''phenomenological model approach'' for PAM and controlled by the ''extended proxy sliding mode'' method. However, the robot is only a trajectory-tracking robot; hence, it is only possible to use it for CPM-type ''passive'' training. In contrast, the antagonistic use of PAM has limitations for rehabilitation use, such as high stiffness owing to the dual PAM structure and slower response. Another limitation is that their range of motion (ROM) outputs are too small to cover the entire range of motion of human joints. There are also robotic devices that use parallel-configured multiple PAM actuators that are individually controlled, such as soft ankle rehabilitation robots [34]. Moreover, exoskeleton-type devices were also implemented, such as ''RUPERT'' which is back-drivable and safe for patients, but the gravity is not compensated and the motion range is limited. It was developed as a passive therapy mode without an active-assist therapy mode [35]. In a recent study, a 4-DOF upper-limb exoskeleton prototype performing trajectory tracking only, which enables the patient to perform passive-mode training, was described in [36]. To avoid the limitations of antagonistic actuation, there are approaches that use single PAM actuation with opposing springs and counterweights [37], [38]. However, most implemented PAM devices focus on trajectory tracking and force control rather than how rehabilitation modes are implemented, and that is limited to ''passive'' training exercises.

A. CONTRIBUTION OF PAPER

To facilitate widespread adoption of rehabilitation, low-cost, highly compliant, and simple-to-operate robotic rehabilitation devices are required. In this study, to provide a novel alternative solution to the aforementioned problem, the following contributions are presented.

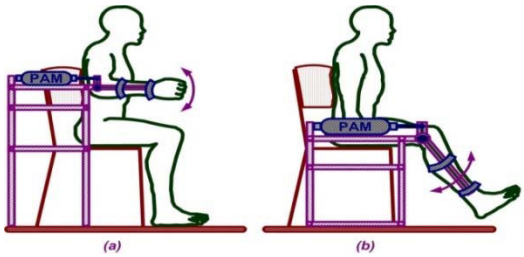


FIGURE 1. Single PAM actuated robotic therapy orthoses proposals. (a) Upper extremity, (b) Lower extremity.

1. A low-cost, highly transparent, single PAM actuated robotic therapy orthosis that enables the patient to perform all training modalities, namely ''passive,'' ''active'' and ''resistive'' is introduced.
2. A novel control approach for robotic orthosis is obtained by combining admittance control and an inverse dynamics-based compliant control approach to form a highly compliant multimodal robotic orthosis implementation for rehabilitation. The novel control approach is a combination of admittance control and the inverse dynamics-based compliant control approach proposed in [38]. A multi-input single-output (MISO) inverse dynamic model implemented by NARX was combined with local cascaded position and pressure PID controllers to obtain a proven solution to the compliant operation of PAM during exercises, with a larger range of motion (ROM) and adaptability to external load impedance variations.
3. By means of simple counterweight loads and compliant control, quasi-static movement of the orthosis resembling isotonic muscle contractions for active exercises is achieved for a full operation range of PAM without any jerky transitions.
4. A new assist-active modality named ''Patient Activated Assistance'' (PAAM) was introduced, in which the patient was the master and the exercise was performed as long as the patient was active. Assistance was provided by sharing load force. The amount of counterweight force reflected on the patient was determined based on the applied gain. This assist-active mode eliminated the slacking problem observed in high-level robotic systems.

The principle diagrams of the proposed single-PAM-actuated robotic therapy orthoses for the upper and lower extremities are shown in Fig. 1.

The remainder of this paper is organized as follows. In Section II, the implementation and methods are provided, and an overview of the robotic orthosis, implemented control approach, and training modalities are explained. Section III presents the experimental results. Section IV presents a discussion.

II. METHODOLOGY

A. OVERVIEW OF THE ROBOTIC ORTHOSIS

In this section, we will explain the overview of the implemented low-cost, highly transparent, single PAM actuated robotic therapy orthosis that enables the patient to perform all training modalities, namely "passive," "active" and "resistive." The orthosis has components such as a mechatronic hardware structure, a graphical user interface (GUI), and compliant control software. The mechatronic hardware structure of the robotic orthosis was formed by adding a patient load arm with a handle and "Velcro" fastening bands to the single PAM-actuated 1 D-o-F robotic device, which was previously developed in [38]. The specifications of the hardware components such as the microcontroller, I/O cards, sensors, valves, PAM, and mechatronic design details are described in [38]. In addition, "Inverse Dynamics Based Compliant Position Controller" is also implemented in the mechatronic structure with demonstrated successful results. The reader is kindly asked to refer to this study for further details. To obtain compliant control software to perform all training modalities, the control approach in [38] was adapted and combined with admittance control. The overall block diagram of the system is shown in Fig.2. The overall block diagram has GUI subsections, namely, the "Therapy Mode Control Panel", "CPM Control Block, and "PAAM Control Block".,The system contains Simulink software blocks for high-level control and for low-level control. Simulink software blocks operate in the microcontroller. The Patient in Therapy also represents the patient connected to the device during the exercise. The GUI sub-sections "CPM Control Block" and "PAAM Control Block" are aimed to enable the therapist to adjust relevant training parameters and "Therapy Mode Control Panel" is used to control the operation of the robotic orthosis. The Therapy Mode Control Panel "Therapy Mode Control Panel" has three sub-sections, "Status" for run-stop control, "Mode Selector" to change the training modalities, and "Manual Position SP" to adjust the position set-point value in manual mode. The robotic therapy device can operate under three different settings. The training modalities consisted of continuous passive exercise (CPM) and patient-activated assistant (PAAM) modalities corresponding to passive, active, and resistive rehabilitation modalities. The manual (MAN) mode is for compliant position control with an adjustable set-point having a fixed position and supplying the reaction force for isometric muscle contraction exercises, and is also utilized for the initial arrangements of the CPM and PAAM modes. When the "Status" is switched to run, the graphical plot screens of each modality are also activated, and the training parameters are recorded.

The prototype rehabilitation devices are preclinical devices, and their performance validation is assessed using healthy subjects and other physiological signals, such as sEMG. A similar approach has been applied in the literature [39], [40], [41]. Therefore, because the implemented robotic orthosis is also a prototype device, the realization of the training modalities is assessed using the sEMG of a healthy person who performs each modality at different times. Biometric data for the person is as follows: Age:18, height 1.80 cm, weight: 90 kg, male. Based on the sEMG results, proper implementation of the training modalities was validated. The implementation of CPM and PAAM modalities is explained in detail in the following sections.

A picture of the single PAM-actuated robotic orthosis during the CPM exercise is shown in Fig.3.

TABLE 1. Orthosis simplified dynamic model variables.

Item	Description	Range / Value
θ_o	Orthosis load arm dynamic angle	-60..+60deg
θ_m	Orthosis measured joint angle	$\theta_m = \theta_o$+180deg
l_1	Orthosis PAM link length	35 mm
l_2	Orthosis patient arm, load arm COM length	150 mm
l_3	Orthosis counterweight COM length	255 mm
l_4	Orthosis load arm to patient handle length	350 mm
τ_o	Orthosis joint torque	0--70N.m
m_w	Orthosis counterweight mass	0.5—3.5 kg
m_a	Approximate mass of patient's forearm	1.5—3.5 kg
m_o	Orthosis load arm mass	0.7 kg
f_o	The load force reflected to PAM	30--1000 N
f_{pam}	The force generated by PAM	0--1000 N
f_m	Orthosis measured total force	0--1000 N
f_p	Applied force via the patient handle	0--100 N
I_{aoz}	Rotational inertia for patient + orthosis load arm	
I_{wz}	Rotational inertia for counterweight	
b_o	Orthosis friction terms coefficient	

B. SIMPLIFIED DYNAMICS OF THE ROBOTIC ORTHOSIS

The robotic orthosis is a 1-D-o-F rotary arm actuated by a single PAM and counterweight. The dynamics of PAM are highly nonlinear and have varying parameters; hence, it was estimated using a model-free adaptive scheme using inverse dynamic properties in our previous work [38]. In the simplified dynamic model of the orthosis, the dynamics of PAM is taken into account as a "black-box" model in connection to the orthosis in terms of measured force and joint position variables. Therefore, the dynamics of the PAM were omitted in the simplified model, and the rest of the orthosis was modeled using a Lagrangian approach.

Fig.4 shows a diagram of the simplified dynamic model with the variables used. Table 1 lists the variables used in this study.

The simplified dynamic model for a robotic orthosis is given in Lagrangian form in the following page, where L is the Lagrange equation, K is the kinetic energy, U is the potential energy, τ is the joint torque, and θ is the joint angle.

$$L = K - U : \tag{1}$$

$$\frac{d}{dt}\frac{\partial L}{\partial \dot{\theta}} - \frac{\partial L}{\partial \theta} = \tau \tag{2}$$

$$K = \frac{1}{2}\left[(m_a + m_o)\, l_2^2 + m_w l_3^2 + I_{aoz} + I_{wz}\right]\dot{\theta}_o^2 \tag{3}$$

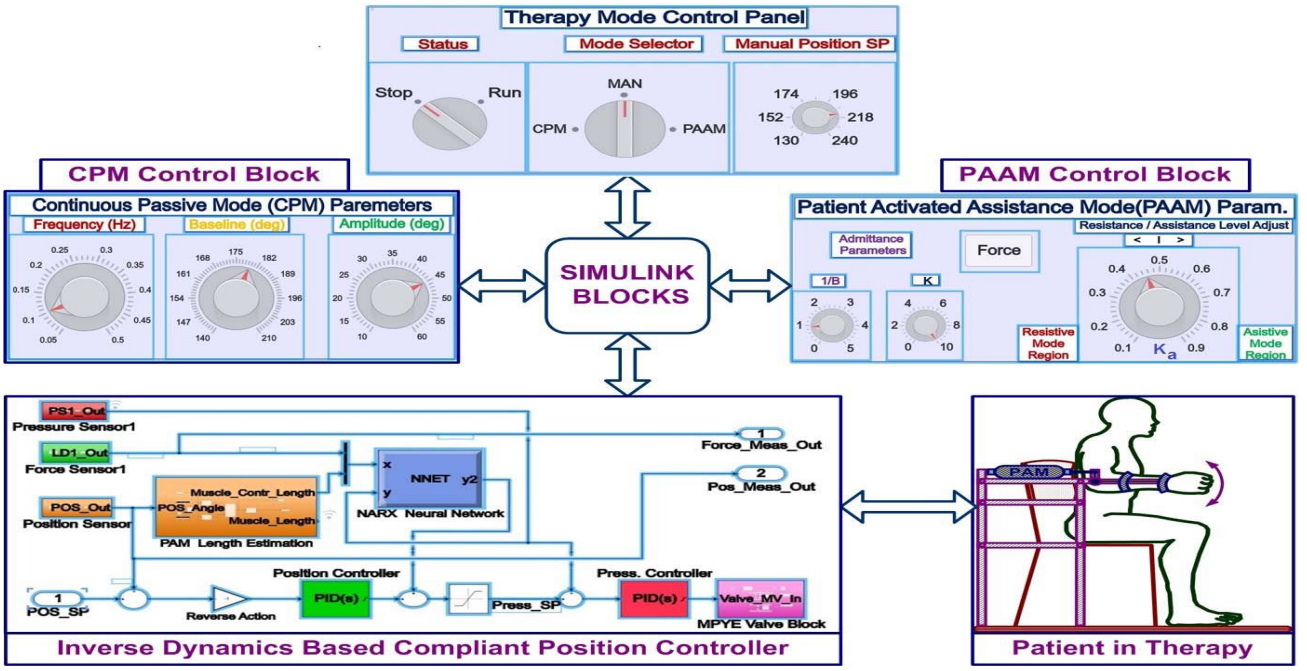


FIGURE 2. Overall block diagram of the PAM actuated therapeutic robotic orthosis.

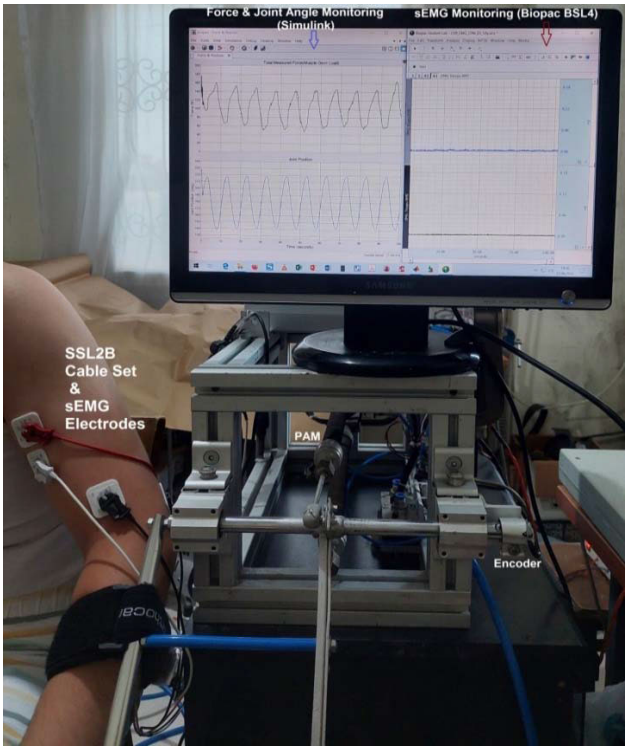


FIGURE 3. Picture of single PAM actuated robotic orthosis during CPM exercise.

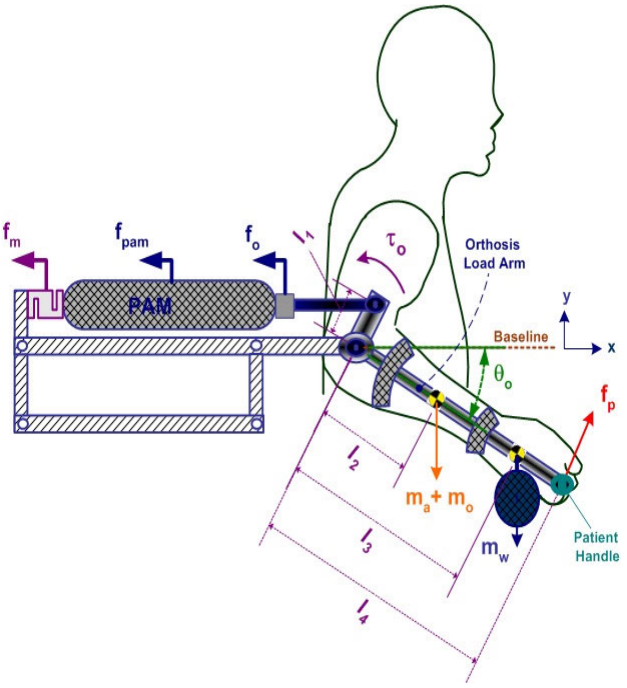


FIGURE 4. Diagram for simplified dynamic model of the orthosis.

$$U = g\left[l_2\left(m_a + m_o\right) + l_3 m_w\right]\left(1 + \sin\theta_o\right) \tag{4}$$

$$\frac{\partial L}{\partial \dot{\theta}_o} = \left[\left(m_a + m_o\right) l_2^2 + m_w l_3^2 + I_{aoz} + I_{wz}\right]\dot{\theta}_o \tag{5}$$

$$\frac{d}{dt}\frac{\partial L}{\partial \dot{\theta}_o} = \left[\left(m_a + m_o\right) l_2^2 + m_w l_3^2 + I_{aoz} + I_{wz}\right]\ddot{\theta}_o \tag{6}$$

$$\frac{\partial L}{\partial \theta} = -g\left[l_2\left(m_a + m_o\right) + l_3 m_w\right]\cos\theta_o \tag{7}$$

$$\frac{d}{dt}\frac{\partial L}{\partial \dot{\theta}_o} - \frac{\partial L}{\partial \theta_o} = \tau_o \tag{8}$$

$$\tau_o = f_o l_1 \cos\theta_o - b_o\dot{\theta}_o + f_p l_4 \tag{9}$$

$$\left[(m_a + m_o)\, l_2^2 + m_w l_3^2 + I_{aoz} + I_{wz}\right]\ddot{\theta}_o + g\,[l_2\,(m_a + m_o) + l_3 m_w]\cos\theta_o = \tau_o \tag{10}$$

Training exercises were performed mainly in isotonic contraction mode. Thus, the robotic orthosis runs in a quasi-static motion, where the rotational velocity of the joint is almost constant and the acceleration is almost zero. Therefore, by neglecting the inertia and bearing friction terms, Equation (10) is reduced to.

$$g\,[l_2\,(m_a + m_o) + l_3 m_w]\cos\theta_o = f_o l_1 \cos\theta_o + f_p l_4 \tag{11}$$

$$f_o = \frac{1}{l_1\cos\theta_o}\left(g\,[l_2\,(m_a + m_o) + l_3 m_w]\cos\theta_o - f_p l_4\right) \tag{12}$$

In quasi-static motion,

$$f_m = f_o + f_{pam} \tag{13}$$

In CPM mode, the patient does not apply any force to the orthosis; therefore, $\mathbf{f_p}$ is almost zero. In the PAAM mode, the patient applies force $\mathbf{f_p}$via the handle as much as possible, depending on the progress of therapy.

C. EMG MEASUREMENT FOR VERIFICATION

The realization of the training modalities was validated by surface EMG measurements using the Biopac Student Lab Physiology Set [42]. The hardware used for the sEMG measurement consisted of a Biopac MP36 data acquisition unit with an SS2LB cable set and electrodes. BSL4 Software was used to monitor and record the data. Measurements were obtained for the Biceps and Triceps. The BSL4 and orthosis high-level Simulink software ran simultaneously during the exercises, recording both the variables and parameters. The rectified RMS values of the signal plots were used to assess the training modality. Verification of the operating modalities using sEMG is also described in the Results section. In Fig 5., a BSL4 recording of the sEMG of the healthy subject was given while performing the active exercise with a 3 kg counterweight, without orthosis operation; that is, the PAM linkage was not connected to the orthosis arm. This measurement was performed to determine the maximum signal level of the measured sEMG to evaluate and compare with the actual sEMG signal levels recorded while the robotic orthosis performed the training modalities.

III. IMPLEMENTATION OF TRAINING MODALITIES

A. BRIEF EXPLANATION OF THERAPY MODALITIES

A brief explanation of the therapeutic modalities is presented for completeness. In ''passive'' mode, during training the subject is passive and does not contribute to the motion whereas the robot is active so that it performs the desired motion, as in continuous passive motion (CPM) devices. CPM training prevents soft tissue stiffening, reduces edema and spasticity as well as passive movements, and generates somatosensory stimulation in afferent neural circuits. On the other hand, in ''active-assisted'' mode, the subject is active and

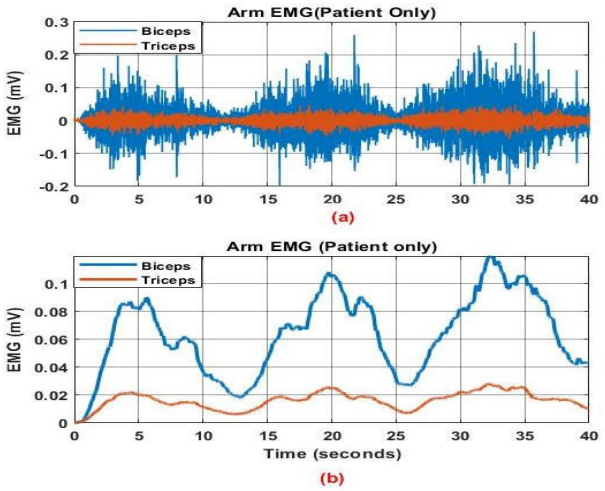


FIGURE 5. sEMG measurement results for the patient performing an exercise with 3kg test load, without robotic orthosis assistance. (a) Raw sEMG result. (b) Rectified RMS signal of part (a), with the peak value of 0.12 mV.

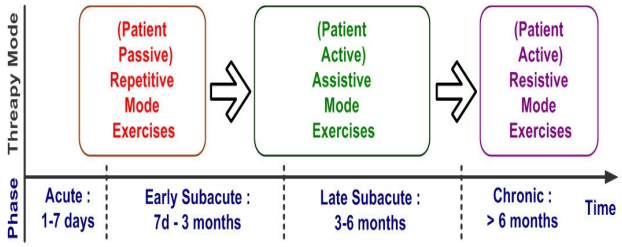


FIGURE 6. The progress of training modalities with respect to phases of stroke, adapted from [3].

tries to complete the motion meanwhile the robot is passive and measures the performance. When the subject is active, motivation for recovery and contribution to motor learning is obtained. Robot-assistance behavior occurs when either weight-counterbalance support or trajectory-based corrective assistance is provided. In this mode, when the subject was unable to complete the task, robot assistance was provided for task completion, during which the subject experienced passive motion. In ''active'' mode, the subject is totally active and tries to complete the task meanwhile the robot is totally passive thru the training period. The robot was only used for performance measurements and did not provide assistance or resistance to the subject. Task completion is not time dependent and depends on the performance of the subject. In ''resistive'' mode, the subject actively performs the task while the robot resists the movement by providing opposing forces against the task completion. During the training stage, the relevant muscles act in an isokinetic mode to enhance muscular strength. To further illustrate how training modalities should be applied during the rehabilitation process, the progress of training modalities with respect to the phases of stroke, adapted from, is shown in Fig. 6, which is adapted from [3].

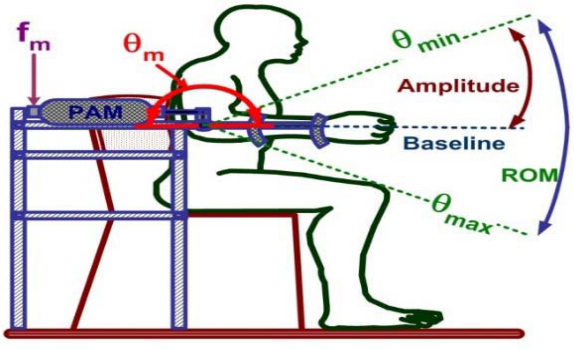


FIGURE 7. Graphical illustration of the system application parameters for CPM mode.

B. CPM MODALITY IMPLEMENTATION

The CPM modality is implemented only for only ''passive'' exercises. Hence, in this modality, the admittance portion of compliant control is not implemented. For implementation, the therapist should adjust the required parameters using a GUI before the exercises begin. The parameters were frequency of exercise, baseline mid-level range of motion (ROM), and amplitude. The baseline approach is illustrated in Fig. 7. During the subacute/acute phase, the therapist determined the trainable section of the limb joint. The therapist selected the desired limb joint ROM segment for the exercise by adjusting the baseline and ROM. Initially, the baseline and amplitude should be adjusted for a very limited ROM, and the frequency should be very low, such as 0.05 Hz. As long as the patient progresses through recovery in CPM, the ROM is increased and the frequency is adjusted. The estimation of the joint angle for exercise is given by Equation (14). The exercise angle formed the trajectory setpoint for the orthosis-compliant position control unit. After the parameter setup is complete, the ''Therapy Mode Selector'' is switched to the CPM position and the ''Status'' is switched to ''Run.'' Then, therapy continues as much as required until ''Status'' is taken to ''Stop.''

$$\theta_{CPM} = \theta_{baseline} + S_{amp} \sin(\omega_o t) \tag{14}$$

C. PAAM MODALITY IMPLEMENTATION

The PAAM modality is implemented for active (assistive and resistive) exercise. Hence, in this modality, the admittance portion of the compliant control is implemented according to the control system block diagram shown in Fig. 8. The combination of admittance control and inverse-dynamics-based compliant control is active in this modality. The admittance control selected was first-order because during experiments and trials, second-order admittance exhibited oscillatory behavior, whereas first-order admittance exhibited robust behavior. Hence, a first-order admittance is implemented as shown in (15). The Simulink admittance control blocks act as the high-level controller whereas the ''Inverse Dynamics Based Compliant Position Controller'' is executed as the low-level controller. The software modules are first transferred to the microcontroller and then run according to the estimated trajectory parameters using GUI settings. For implementation, the therapist should adjust the required parameters using a GUI before the exercises begin. The required parameters for the PAAM modality are F_ref, Ka, B, and K. Ka is the admittance gain used in the reflected force estimation. For the range of Ka ''0.9-0.5'', the robotic orthosis behaves as ''assistive'', whereas for the range of ''0.5-0.1'', it behaves as ''resistive''. B and K are the admittance adjustment parameters given in (15). The conversion method for the force to position is given by Eqs.(17) and (18). Ka, B, and K were adjusted before PAAM training using GUI knobs. F_ref is the gravitational reference force corresponding to the orthosis load arm weight and counterweight. After the patient was connected to the load arm, the PAAM exercise was started. First, the ''Therapy Mode Selector'' is switched to ''Manual'' mode, and the manual position set-point is adjusted to approximately 175..180 deg. After the orthosis reached the set point and while it is standstill, the ''Force'' button in the PAAM control panel is pressed and a reference value for the f_o given in (12) is obtained via the force sensor. The operation of the orthosis in the PAAM modality is as follows. After parameter adjustment is completed by the therapist, the ''Therapy Mode Selector'' is switched to ''PAAM'' and ''Status'' is switched to ''Run''. The robot waits for the patient to apply a force to the handle according to the desired motion direction. The block diagram of the PAAM control system shown in Fig. 8 converts the force applied on the orthosis handle into an incremental motion request. The compliant position controller then moves the orthosis accordingly. The therapy continues as long as the patient applies force to the orthosis handle and is repeated cyclically in the upward and downward directions. Whenever the patient stopped applying force, the exercise was paused. After the pause, if the patient again applied force to the handle, the exercise was continued from the last point. This modality is exercised as much as required until ''Status'' is taken to ''Stop.'' Symbols used in the PAAM modality control system is given in Table 2.

The first-order admittance control for the rotary joint of the orthosis is given by (15).

$$\theta_a(s) = \frac{1}{(Bs + K)} \tau_a(s) \tag{15}$$

By substituting the inverse Laplace and submitting force variables into (15), we obtain the following differential equations, given in (16) and (17):

$$B\dot{\theta}_a + K\theta_a = l_1 f_a(t) \tag{16}$$

$$B\dot{\theta}_a + K\theta_a = l_1 \left[f_m(t) - F_ref\,(t)\right] \tag{17}$$

When (17) is discretized with the control system sampling time **Ts**, the following forms are obtained: (18),(19), and (20), where ***k*** is the discrete time step for the overall control system:

$$\dot{\theta}_a(\mathrm{t}) \cong \frac{\theta_a(k) - \theta_a(k-1)}{T_s} \tag{18}$$

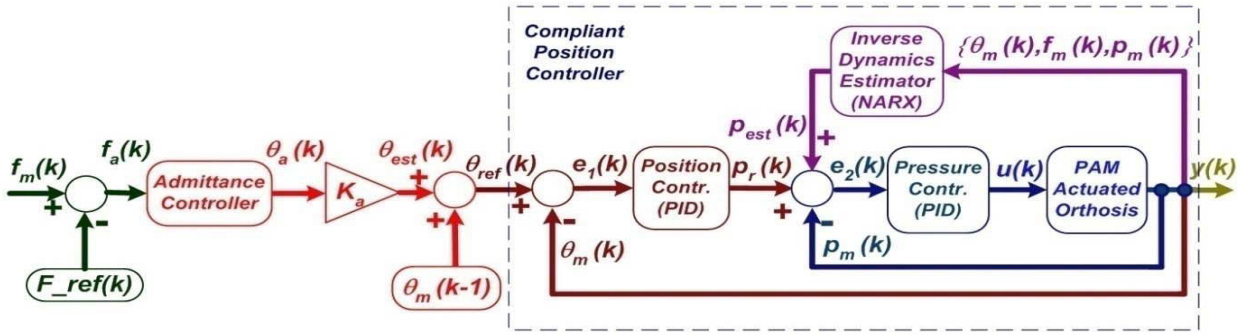


FIGURE 8. PAAM modality control system block diagram of the therapeutic robotic orthosis.

TABLE 2. Symbols used in the proposed PAAM mode control system.

Symbol	Meaning
$\theta_{est}(k)$	The estimated joint position value
$\theta_m(k)$	Orthosis arm measured current joint position angle
$\theta_m(k\text{-}1)$	Orthosis arm measured previous joint position angle
$\theta_a(k)$	The admittance block estimated joint position value
$f_a(k)$	The admittance block input force
F_ref(k)	Orthosis reference force for counterweight load
$\theta_{ref}(k)$	The position control loop reference value
$e_1(k)$	Position control loop error
$p_r(k)$	Pressure loop reference value from position controller
$p_{est}(k)$	Pressure feedback value from Inverse Dynamics Estimator
$e_2(k)$	Pressure control loop error
u(k)	Pressure controller output
y(k)	Orthosis output
$p_m(k)$	PAM applied pressure
$f_m(k)$	Orthosis measured force (PAM gen.+ load)

$$\theta_a(k) = \theta_a(k-1) + \left[\frac{T_s}{B}\{l_1\,(f_m(k) - F_ref\,(k)) - K\theta_a(k)\}\right] \quad (19)$$

$$\theta_{ref}(k) = K_a\theta_a(k) + \theta_m(k-1) \quad (20)$$

IV. RESULT

A. CPM TRAINING RESULTS

In this section, the results obtained during the CPM modality training implementation are presented. At this point, for the sake of clarity, a brief implementation perspective of the CPM exercises is provided. As indicated in the previous sections, the CPM modality was applied to a patient in either the acute or subacute phase of the recovery process. Hence, the patient was completely passive, and the training exercises were performed using the robotic orthosis according to the parameters set by the therapist. The force contribution of the patient to the orthosis was almost zero, and the robotic device estimated the trajectory using compliant position control in accordance with the load force. The load force is composed of gravitational components of the forearm, orthosis hardware, and counterweights, which are determined by force measurements. During the CPM exercise, to achieve quasi-static motion, the compliant position control system for the PAM generates an amount of force to overcome the limb stiffness, in addition to the load force. The measured force is the sum of the load force and the force generated by the PAM.

In this study, CPM exercise implementation variants were performed on the same subject. To demonstrate that the implementation ran for different subjects with varying forearm loads, the exercises were performed with varying counterweights and frequencies. Under normal clinical conditions, CPM exercises are performed using only the patient limb loads without additional counterweights.

In Fig. 9, the CPM therapy exercise performance results at a 0.1 Hz frequency of 80 deg. ROM is given successively as in (a) result for the only forearm load, in (b) result with forearm load + 0.5 kg counterweight and (c) forearm load+ 1.0 kg counterweight. In Fig. 10, the CPM therapy exercise performance results for the 0.25 Hz frequency and 80 °ROM are shown successively as (a) result for only forearm load, (b) result with forearm load + 0.5 kg counterweight, and (c) result with forearm load + 1.0 kg counterweight. In all of them, Biceps & Triceps EMG measurements were also approximately zero (≅0.0025mV), which indicates that the patient's muscles were passive during the exercise at both 0.1 Hz and 0.25 Hz frequencies.

The limited ROMs are shown in Fig. 11. For example, in (a), the baseline shifted to 160 °. and with a 50 deg. The ROM exercises were performed at 0.1 Hz. Moreover, as shown in (b), the baseline shifted to 190 °. and 40 deg. The ROM exercises were performed at 0.25 Hz. EMG measurements of the biceps and triceps were close to zero (≅ 0.0025mV), indicating that the patient's muscles were passive.

Although 0.5 and 1 kg counterweight loads were added to the robotic orthosis load arm, the Biceps & Triceps EMG measurements remained very close to zero in the range of 0.001–0.0025 mV. This indicates that the patient's muscles

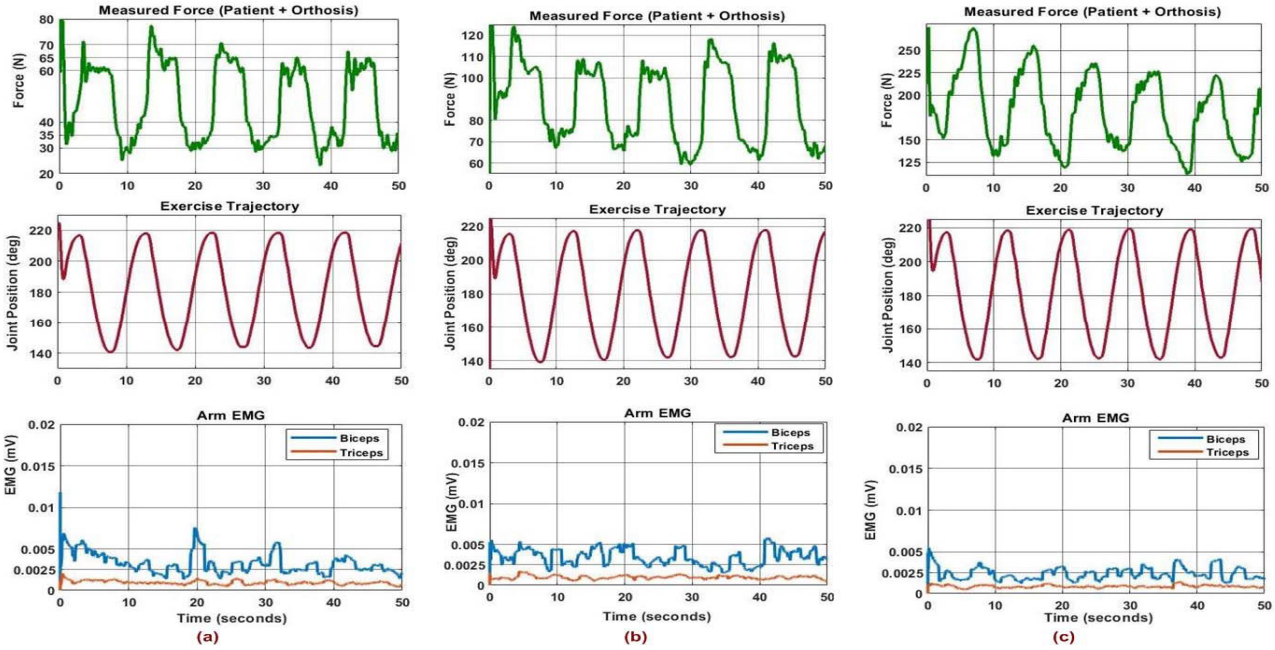


FIGURE 9. CPM therapy exercise performance results, (0.1 Hz & 80 deg. ROM): (a) with only forearm load, (b) with forearm load + 0.5kg counterweight, (c) with forearm load + 1.0kg counterweight.

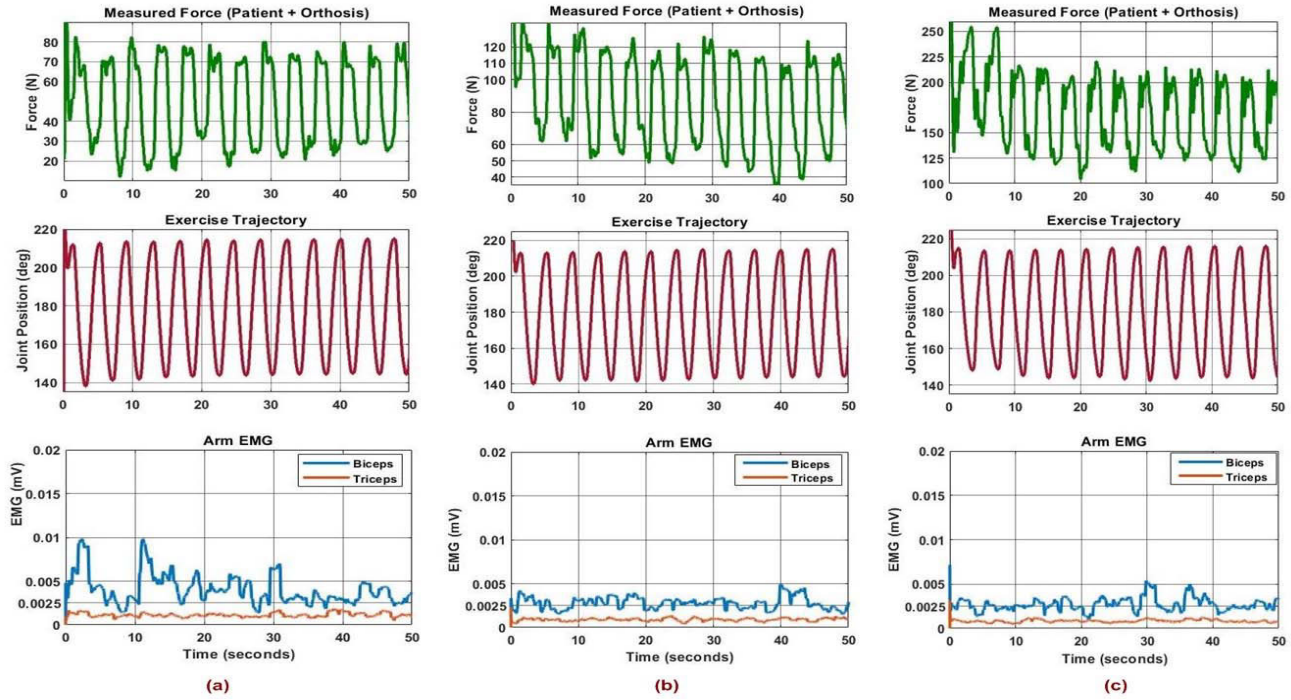


FIGURE 10. CPM therapy exercise performance results, (0.25 Hz & 80 deg. ROM): (a) with only forearm load, (b) with forearm load + 0.5kg counterweight, (c) with forearm load + 1.0kg counterweight.

were passive during all the exercises. In this way, the proper implementation of the CPM modality was validated by the invariance of the EMG level in the no-load and additional load cases. In all cases, the loads were compensated by a robotic orthosis powered by PAM.

In general, the exercise results demonstrated the proper implementation of CPM therapy exercises with respect to different frequencies, varying patient forearms, and the desired ROM for the limb using the proposed robotic orthosis and control method.

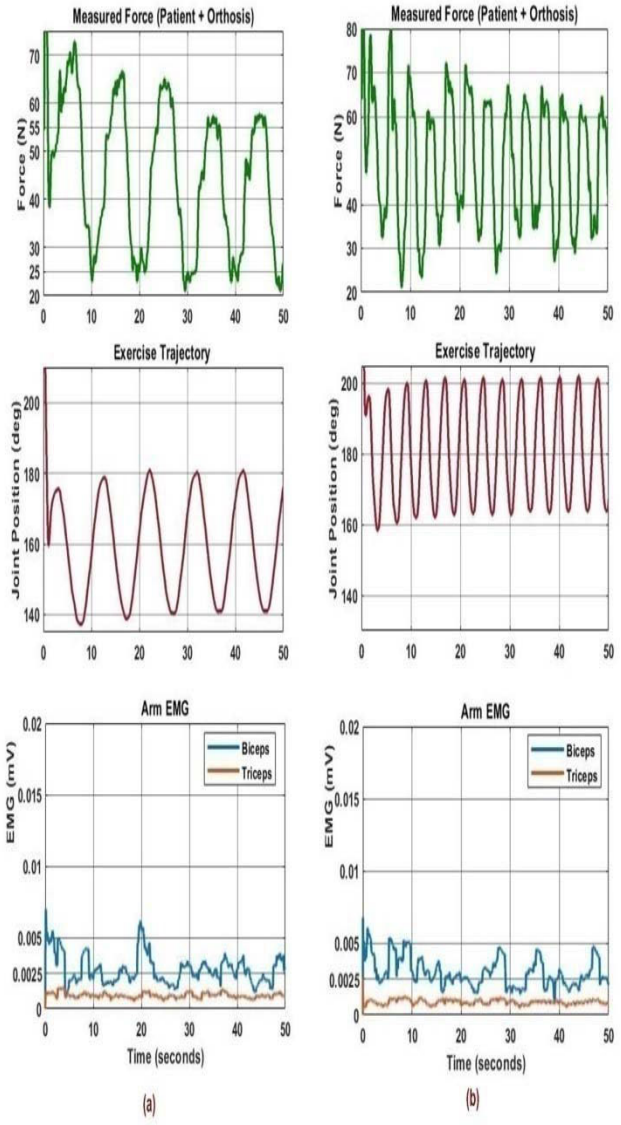


FIGURE 11. CPM therapy exercise performance results for baseline shifts and limited ROMs: (a) Baseline shifted to 160 deg. and 50 deg. ROM 0.1Hz exercise, (b) Baseline shifted to 190 deg. and 40 deg. ROM 0.25 Hz exercise.

B. PAAM TRAINING RESULTS

In this section, PAAM modality therapy exercise performance results are presented. The PAAM modality is implemented for active (assistive and resistive) exercise. As indicated in the previous sections, the PAAM modality is applied to a patient in the late subacute or chronic phase of the recovery process. Hence, the patient was active, the training exercises were performed by the patient, and the robotic orthosis facilitated the training according to the parameters set by the therapist. The patient performed the exercise by applying force on the handle in the desired direction of motion. This force results in an incremental motion request. The therapy continues as long as the patient applies force to the orthosis handle, and is repeated cyclically in the upward and downward directions. Whenever the patient stopped applying force to the handle, the exercise was paused. After the pause, if the patient again applied force to the handle, the exercise was continued from the last point. During the PAAM exercise, motion characteristics such as ROM, exercise speed, and frequency were based on the patient's performance. The force contribution of the patient to the training exercise was estimated in accordance with Ka, the admittance gain, which is the gain used in reflected force estimation and load sharing. For the Ka range of 0.9-0.5, the robotic orthosis behaves as ''assistive'', whereas for the range of 0.5-0.1, it behaves as ''resistive''.

In this study, variants of the PAAM exercise were performed by the same subject. To demonstrate that the implementation ran for different subjects with varying forearm loads, exercises were performed with varying counterweights. At this point, it may be useful to re-express that there is a ratio of 10 between the orthosis force (f_o) and the force applied to the patient handle (f_p) owing to the (l_4/l_1) lever gain. Hence, the patient sensed 10 % of the measured force on the orthosis. During the exercises, to obtain a rough index figure for the amount of force that the patient contributed, a relative variable f_{index} is introduced, which was estimated using (21), where f_{max} and f_{min} were determined from the relevant force graph.

$$f_{index} \cong (f_{max} - f_{min}) \tag{21}$$

Fig. 12 shows the PAAM therapy mode performance results with an additional counterweight of 1 kg. The admittance parameters, B=1 and K=10, were adjusted via the GUI, and F_ref=125N was estimated before the exercise. The force index and EMG peak variation with the Ka gain are listed in Table 3.

In Fig. 13, the PAAM therapy mode performance results with a 3 kg additional counterweight load are shown. The admittance parameters, B=1 and K=10, were adjusted via the GUI, and F_ref=305N was estimated before the exercise. The force index and EMG peak variation with the Ka gain are listed in Table 4.

When the results given in Tables 3 and 4 were inspected, it was observed that the force index increased as the Ka gain decreased, indicating that the patient experienced smaller forces with high Ka gains and larger forces with low Ka gains. Therefore, a variation in Ka from higher to lower values enables the therapy modality to switch from assistance to resistance.

The verification of the PAAM implementation was performed using EMG levels of the Biceps and Triceps, as Ka varied. In Fig. 12 and 13, the plots of the EMG signals recorded during the training exercises for different Ka values ranging from 0.9 0.1. The EMG peak values are also given in Tables 3 and 4 for quick evaluation. A situation similar to that of the force index occurs for the EMG levels. In both Fig.12 and Fig.13 plots and in Tables 3 and 4, it was observed that the EMG levels (peaks) increased as the Ka gain decreased, meaning that the patient experienced smaller forces with high Ka gains and larger forces with low Ka

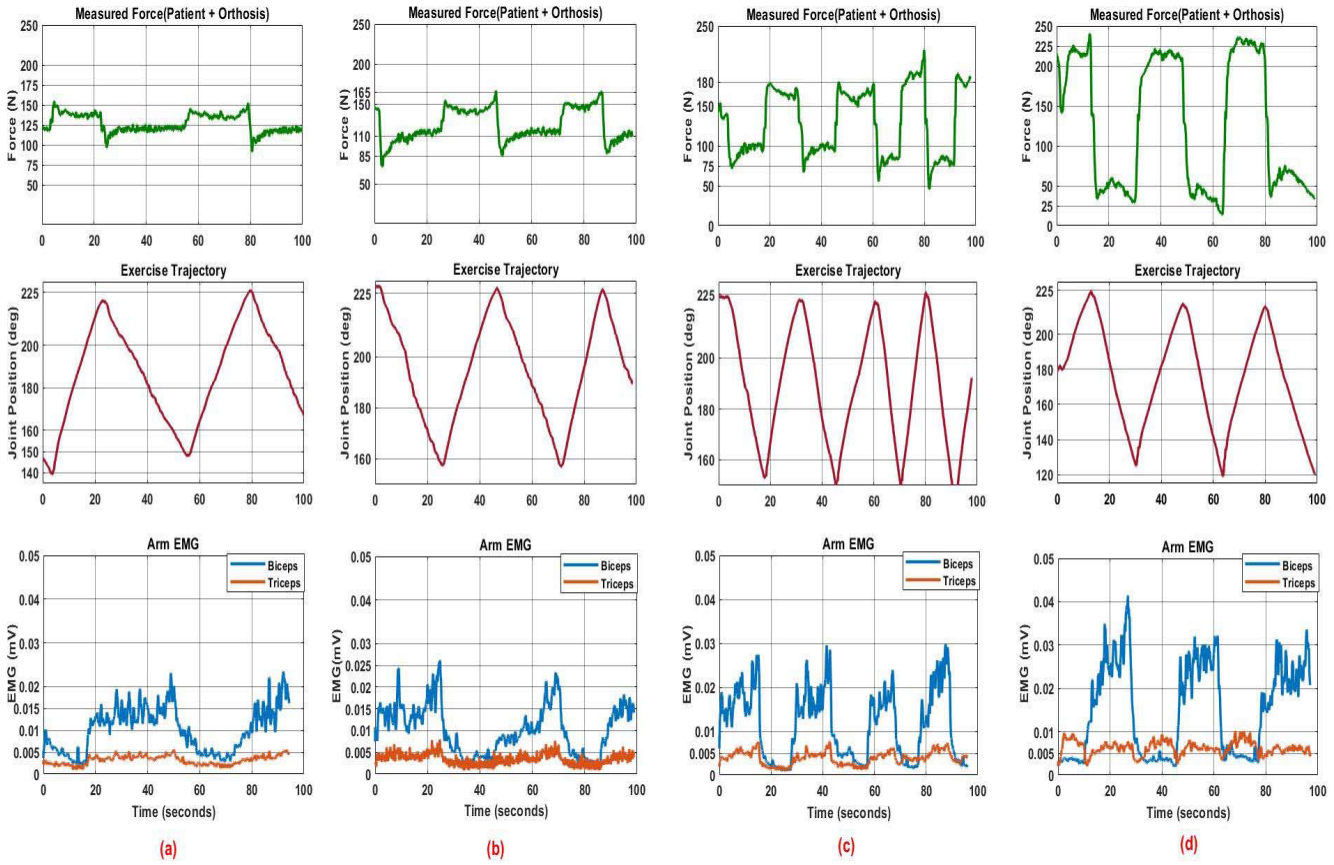


FIGURE 12. PAAM therapy mode performance results with 1kg additional counterweight load: (a) exercise with Ka = 0.9 gain value, (b) exercise with Ka = 0.6 gain value, (c) exercise with Ka = 0.35 gain value, (d) exercise with Ka = 0.1 gain value.

TABLE 3. Force index and EMG peak variation with Ka gain, for 1kg counterweight load, F_ref =125 N.

Fig. 12 Parts	(a)	(b)	(c)	(d)
Ka=	0.9	0.6	0.35	0.1
f_{index} (N) $\cong$	50	80	110	200
EMG peaks (mV) (Bic /Tri)	0.02 / 0.004	0.025 / 0.006	0.03 / 0.007	0.04/ 0.01

TABLE 4. Force index and EMG peak variation with the Ka gain, for 3kg counterweight load, F_ref = 305 N.

Fig. 13 Parts	(a)	(b)	(c)	(d)
Ka =	0.9	0.6	0.35	0.1
f_{index} (N) $\cong$	100	175	300	500
EMG peaks (mV) (Bic / Tri)	0.03 / 0.015	0.045/ 0.02	0.06 /0.03	0.08 / 0.05

gains. As a result, lower EMG levels were recorded with high Ka values, indicating that the PAAM was in assistance mode, and higher EMG levels were recorded with low Ka values, indicating that the PAAM was in resistance mode. It is also noteworthy that a difference in EMG levels for the Triceps and Biceps occurs with respect to the applied force direction (up or down). The biceps generate a patient force in the upward direction, whereas the triceps generate a patient force in the downward direction. In the upward direction, the patient force is against gravity; hence, to start the motion, it should overcome a portion of the orthosis load force to trigger motion control, which requires some effort. On the other hand, for down motion, the patient force is along gravity; hence, to start down motion, a small amount of effort is required to trigger motion control. This situation is particularly evident with a high Ka gain. As Ka decreases, the difference decreases to a reasonable level. To train the triceps further, the therapy was implemented in resistive mode while the patient applied a down-pushing force to the handle.

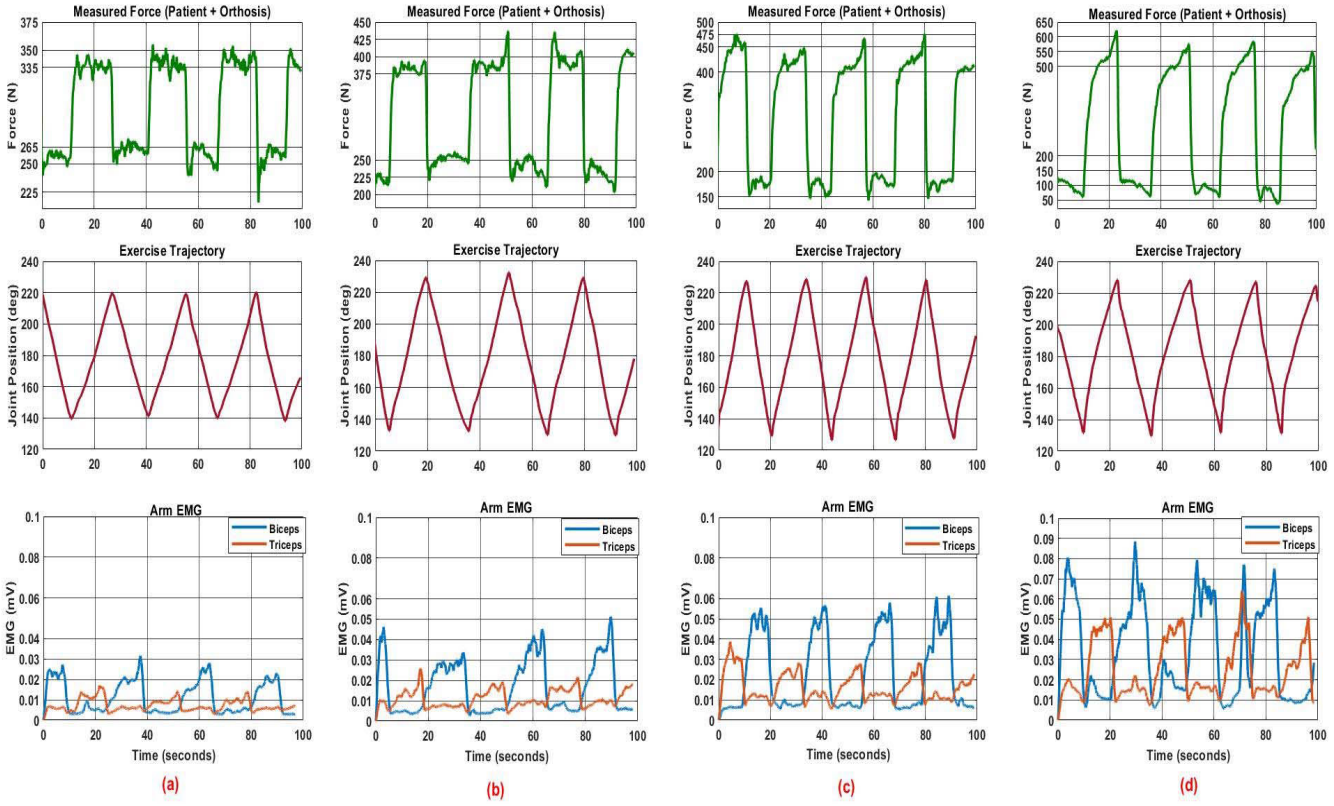


FIGURE 13. PAAM therapy mode performance results with 3kg additional counterweight load: (a) exercise with Ka = 0.9 gain value, (b) exercise with Ka = 0.6 gain value, (c) exercise with Ka = 0.35 gain value, (d) exercise with Ka = 0.1 gain value.

In conclusion, the results demonstrated that EMG levels increase as Ka varies from higher to lower values, verifying that the therapy modality has been properly implemented to switch from assistance to resistance range.

In Fig. 14, the PAAM therapy performance results with patient pauses demonstrating transparency are shown under an additional counterweight load of 2 kg. In (a), the exercise was performed with a 0.35 gain value of, and in (b) with a 0.6 gain value. In (a), the region marked as ''I'' indicates the first pause of the patient for approximately 10 s. During this pause, the patient releases the handle. The trajectory plot was stationary at 225 °, indicating that the orthosis had not been moving, and the force plot indicated that the measured force was equal to F_ref=230 N. The EMG levels decreased below 0.005 mV, verifying that the patient did not apply any force. The region marked as ''II'' indicates the second pause of the patient for approximately 11 s. A situation similar to that of the previous pause was observed. However, since the patient had released the handle at an upper position, to continue after the second pause, the patient first raised the arm upward and then touched the handle, which resulted in a biceps contraction marked as ''P'' in the plot. In (b), similar patient pauses were demonstrated with shorter durations and higher Ka values, as indicated by regions ''III'' and ''IV.'' In this case, it was also demonstrated that the orthosis in the PAAM mode was completely under the control of the patient and was highly transparent. It did not make No action was taken after the patient stopped. It became active after the patient started the training.

C. MODALITY TRANSITION ACCORDING TO THERAPY SEQUENCE

In this section, the proposal for the therapy modality transition is implemented by the robotic orthosis in accordance with the timeline shown in Fig.6. In this study, CPM therapy was initiated during the acute and early sub-acute phases. It was converted to PAAM in the late subacute phase as an assistive starting with Ka=0.9. Assistance gradually decreased as neuromuscular recovery developed until Ka=0.5. In the chronic phase, PAAM acts as a resistive mode starting with Ka=0.5 and it ends with Ka=0.1. An example of a modality transition is shown in Fig. 15.

V. DISCUSSION

In this work, a low-cost, highly transparent, single PAM actuated robotic therapy orthosis that enables the patient to perform all training modalities, namely ''passive,'' ''active'' and ''resistive'' was presented. An alternative solution is to support the widespread adoption of rehabilitation and simple-to-operate robotic rehabilitation devices. The approximate cost of the proposed prototype device was around 1.5k USD.

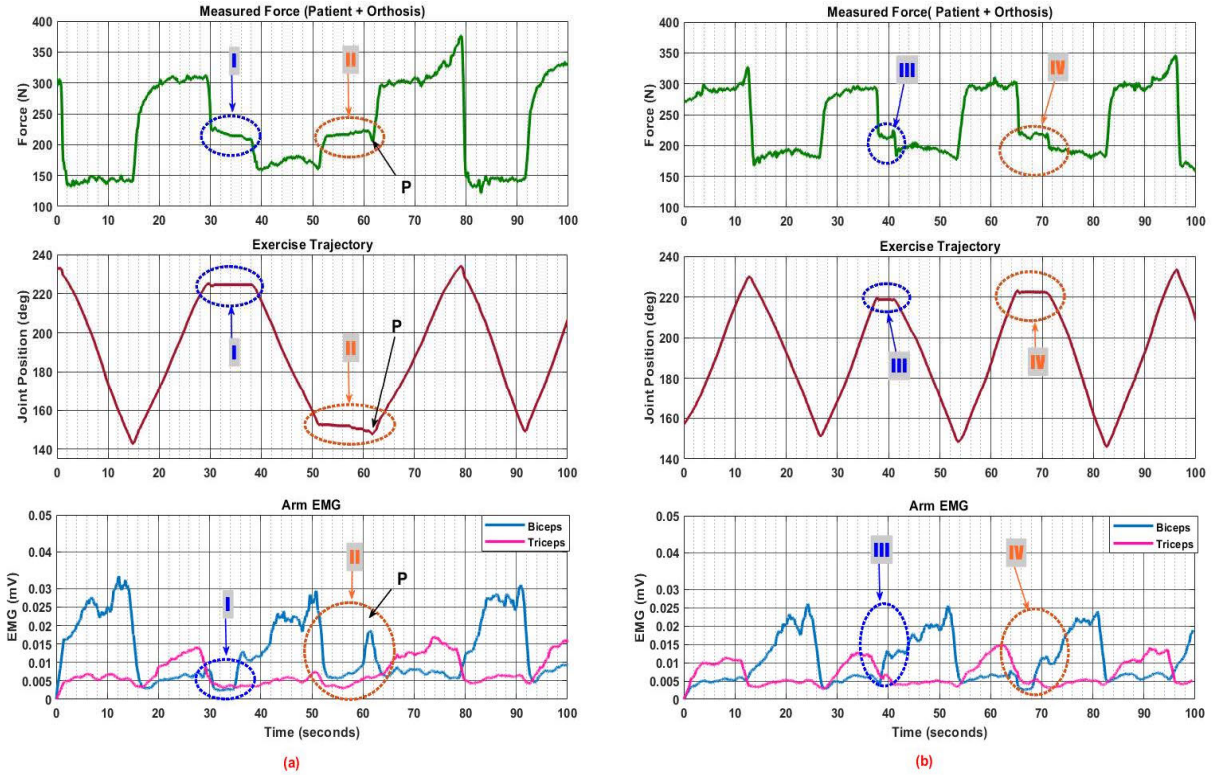


FIGURE 14. PAAM therapy performance results with patient pauses demonstrating transparency, under 2kg additional counterweight load. (a) exercise with 0.35 gain value. (b) exercise with 0.6 gain value.

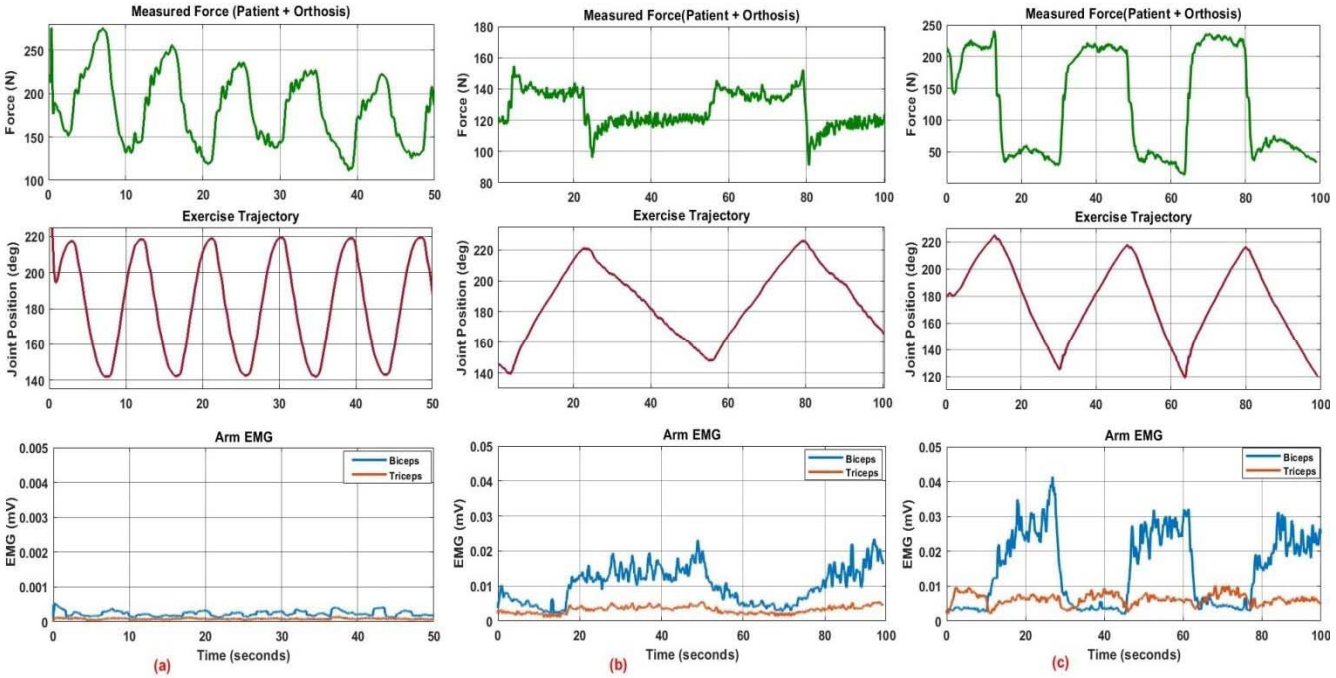


FIGURE 15. Modality transition from CPM to PAAM (Assistive, Resistive) therapy performance, under 1kg additional counterweight load. (a) CPM exercise, (b) PAAM exercise with 0.9 gain value (assistive), (c) PAAM exercise with 0.1 gain value(resistive).

The main contributions of this study are as follows: First, a novel control approach for the robotic orthosis was obtained by combining admittance control and an inverse dynamics-based compliant control approach to form a highly compliant multimodal robotic orthosis implementation. In addition, by means of simple counterweight loads

and compliant control, quasi-static movement of the orthosis resembling isotonic muscle contractions for active exercises was obtained for a full operation range of PAM without any jerky transitions. The counterweight approach is simple enough to implement without any technical support, as compared to the spring return single PAM-based devices, where the adjustment of spring stiffness is very difficult and requires technical assistance. Furthermore, a new assist-active modality named ''Patient Activated Assistance'' (PAAM) was demonstrated, in which the patient was the master and the exercise was performed as long as the patient had been active. Assistance was provided by sharing the load force. The amount of counterweight force reflected on the patient was determined based on the applied gain. This assist-active mode eliminated the slacking problem observed in high-level robotic systems. To summarize, the obtained results could also used to justify performance validation. For instance, adjustable ROM and region for trajectories and almost zero sEMG values with respect to different weights indicate the proper passive CPM modality. Furthermore, proportional variation of sEMG values with respect to Ka variation proves the implementation of the patient-assisted active mode, as well as patient-determined ROM and speed of exercise demonstrated transparency.

The training modality implementations could be seen in the annexed videos.

Although the proposed approach was lacking for game-based graphical simulations, the successful results demonstrated that it could directly be a solution for ''proprioception deficit'' recovery in which the visual factors are eliminated on purpose. According to [43], ''In subjects with both proprioceptive and motor impairments, assistive exercise might be more effective if at least part of the training were performed without vision.''

In conclusion, the results demonstrated that the proposed low-cost single-PAM-actuated robotic orthosis could be a solution to robotic rehabilitation demands, especially in low-middle-income countries (LMIC). For future works, this approach could be extended to different mechanisms and higher D-o-F devices.

REFERENCES

[1] V. L. Feigin, M. Brainin, B. Norrving, S. Martins, R. L. Sacco, W. Hacke, M. Fisher, J. Pandian, and P. Lindsay, ''World stroke organization (WSO): Global stroke fact sheet 2022,'' *Int. J. Stroke*, vol. 17, no. 1, pp. 18–29, Jan. 2022, doi: 10.1177/17474930211065917.

[2] J. Young and A. Forster, ''Review of stroke rehabilitation,'' *BMJ*, vol. 334, no. 7584, pp. 86–90, Jan. 2007, doi: 10.1136/bmj.39059.456794.68.

[3] J. Bernhardt, K. S. Hayward, G. Kwakkel, N. S. Ward, S. L. Wolf, K. Borschmann, J. W. Krakauer, L. A. Boyd, S. T. Carmichael, D. Corbett, and S. C. Cramer, ''Agreed definitions and a shared vision for new standards in stroke recovery research: The stroke recovery and rehabilitation roundtable taskforce,'' *Int. J. Stroke*, vol. 12, no. 5, pp. 444–450, Jul. 2017, doi: 10.1177/1747493017711816.

[4] S. Dehem, M. Gilliaux, G. Stoquart, C. Detrembleur, G. Jacquemin, S. Palumbo, A. Frederick, and T. Lejeune, ''Effectiveness of upper-limb robotic-assisted therapy in the early rehabilitation phase after stroke: A single-blind, randomised, controlled trial,'' *Ann. Phys. Rehabil. Med.*, vol. 62, no. 5, pp. 313–320, Sep. 2019, doi: 10.1016/j.rehab.2019.04.002.

[5] V. S. Huang and J. W. Krakauer, ''Robotic neurorehabilitation: A computational motor learning perspective,'' *J. NeuroEng. Rehabil.*, vol. 6, no. 1, pp. 1–13, Feb. 2009, doi: 10.1186/1743-0003-6-5.

[6] F. Molteni, G. Gasperini, G. Cannaviello, and E. Guanziroli, ''Exoskeleton and end-effector robots for upper and lower limbs rehabilitation: Narrative review,'' *PM&R*, vol. 10, no. 9, pp. S174–S188, Sep. 2018, doi: 10.1016/j.pmrj.2018.06.005.

[7] J. Mehrholz, M. Pohl, T. Platz, J. Kugler, and B. Elsner, ''Electromechanical and robot-assisted arm training for improving activities of daily living, arm function, and arm muscle strength after stroke,'' *Cochrane Database Systematic Rev.*, vol. 2018, no. 9, Sep. 2018, Art. no. CD006876, doi: 10.1002/14651858.CD006876.pub5.

[8] M. Franceschini, S. Mazzoleni, M. Goffredo, S. Pournajaf, D. Galafate, S. Criscuolo, M. Agosti, and F. Posteraro, ''Upper limb robot-assisted rehabilitation versus physical therapy on subacute stroke patients: A follow-up study,'' *J. Bodywork Movement Therapies*, vol. 24, no. 1, pp. 194–198, Jan. 2020, doi: 10.1016/j.jbmt.2019.03.016.

[9] L. Zhang, G. Jia, J. Ma, S. Wang, and L. Cheng, ''Short and long-term effects of robot-assisted therapy on upper limb motor function and activity of daily living in patients post-stroke: A meta-analysis of randomized controlled trials,'' *J. NeuroEng. Rehabil.*, vol. 19, no. 1, pp. 1–22, Jul. 2022, doi: 10.1186/s12984-022-01058-8.

[10] J. Wu, H. Cheng, J. Zhang, S. Yang, and S. Cai, ''Robot-assisted therapy for upper extremity motor impairment after stroke: A systematic review and meta-analysis,'' *Phys. Therapy*, vol. 101, no. 4, Apr. 2021, Art. no. pzab010, doi: 10.1093/ptj/pzab010.

[11] I. Carpinella, T. Lencioni, T. Bowman, R. Bertoni, A. Turolla, M. Ferrarin, and J. Jonsdottir, ''Effects of robot therapy on upper body kinematics and arm function in persons post stroke: A pilot randomized controlled trial,'' *J. NeuroEng. Rehabil.*, vol. 17, no. 1, p. 10, Jan. 2020, doi: 10.1186/s12984-020-0646-1.

[12] K. Moulaei, K. Bahaadinbeigy, A. A. Haghdoostd, M. S. Nezhad, and A. Sheikhtaheri, ''Overview of the role of robots in upper limb disabilities rehabilitation: A scoping review,'' *Arch. Public Health*, vol. 81, no. 1, p. 84, May 2023, doi: 10.1186/s13690-023-01100-8.

[13] R. Iandolo, F. Marini, M. Semprini, M. Laffranchi, M. Mugnosso, A. Cherif, L. De Michieli, M. Chiappalone, and J. Zenzeri, ''Perspectives and challenges in robotic neurorehabilitation,'' *Appl. Sci.*, vol. 9, no. 15, p. 3183, Aug. 2019, doi: 10.3390/app9153183.

[14] P. Maciejasz, J. Eschweiler, K. Gerlach-Hahn, A. Jansen-Troy, and S. Leonhardt, ''A survey on robotic devices for upper limb rehabilitation,'' *J. NeuroEngineering Rehabil.*, vol. 11, no. 1, pp. 1–29, Jan. 2014, doi: 10.1186/1743-0003-11-3.

[15] R. Fareh, A. Elsabe, M. Baziyad, T. Kawser, B. Brahmi, and M. H. Rahman, ''Will your next therapist be a robot?—A review of the advancements in robotic upper extremity rehabilitation,'' *Sensors*, vol. 23, no. 11, p. 5054, May 2023, doi: 10.3390/s23115054.

[16] I. Díaz, J. J. Gil, and E. Sánchez, ''Lower-limb robotic rehabilitation: Literature review and challenges,'' *J. Robot.*, vol. 2011, pp. 1–11, Nov. 2011, doi: 10.1155/2011/759764.

[17] D. Pinto-Fernandez, D. Torricelli, M. D. C. Sanchez-Villamanan, F. Aller, K. Mombaur, R. Conti, N. Vitiello, J. C. Moreno, and J. L. Pons, ''Performance evaluation of lower limb exoskeletons: A systematic review,'' *IEEE Trans. Neural Syst. Rehabil. Eng.*, vol. 28, no. 7, pp. 1573–1583, Jul. 2020, doi: 10.1109/TNSRE.2020.2989481.

[18] A. Basteris, S. M. Nijenhuis, A. H. Stienen, J. H. Buurke, G. B. Prange, and F. Amirabdollahian, ''Training modalities in robot-mediated upper limb rehabilitation in stroke: A framework for classification based on a systematic review,'' *J. NeuroEng. Rehabil.*, vol. 11, no. 1, p. 111, 2014, doi: 10.1186/1743-0003-11-111.

[19] S. D. Gasperina, L. Roveda, A. Pedrocchi, F. Braghin, and M. Gandolla, ''Review on patient-cooperative control strategies for upper-limb rehabilitation exoskeletons,'' *Frontiers Robot. AI*, vol. 8, Dec. 2021, Art. no. 745018, doi: 10.3389/frobt.2021.745018.

[20] T. Proietti, V. Crocher, A. Roby-Brami, and N. Jarrassé, ''Upper-limb robotic exoskeletons for neurorehabilitation: A review on control strategies,'' *IEEE Rev. Biomed. Eng.*, vol. 9, pp. 4–14, 2016, doi: 10.1109/RBME.2016.2552201.

[21] Q. Miao, M. Zhang, J. Cao, and S. Q. Xie, ''Reviewing high-level control techniques on robot-assisted upper-limb rehabilitation,'' *Adv. Robot.*, vol. 32, no. 24, pp. 1253–1268, Dec. 2018, doi: 10.1080/01691864.2018.1546617.

[22] M. Schumacher, J. Wojtusch, P. Beckerle, and O. von Stryk, "An introductory review of active compliant control," *Robot. Auto. Syst.*, vol. 119, pp. 185–200, Sep. 2019, doi: 10.1016/j.robot.2019.06.009.
[23] A. Calanca, R. Muradore, and P. Fiorini, "A review of algorithms for compliant control of stiff and fixed-compliance robots," *IEEE/ASME Trans. Mechatronics*, vol. 21, no. 2, pp. 613–624, Apr. 2016, doi: 10.1109/TMECH.2015.2465849.
[24] P. Song, Y. Yu, and X. Zhang, "A tutorial survey and comparison of impedance control on robotic manipulation," *Robotica*, vol. 37, no. 5, pp. 801–836, May 2019, doi: 10.1017/S0263574718001339.
[25] A. Q. Keemink, H. van der Kooij, and A. H. Stienen, "Admittance control for physical human–robot interaction," *Int. J. Robot. Res.*, vol. 37, no. 11, pp. 1421–1444, Sep. 2018, doi: 10.1177/0278364918768950.
[26] L. Li, S. Tyson, and A. Weightman, "Professionals' views and experiences of using rehabilitation robotics with stroke survivors: A mixed methods survey," *Frontiers Med. Technol.*, vol. 3, Nov. 2021, Art. no. 780090, doi: 10.3389/fmedt.2021.780090.
[27] G. Turchetti, N. Vitiello, L. Trieste, S. Romiti, E. Geisler, and S. Micera, "Why effectiveness of robot-mediated neurorehabilitation does not necessarily influence its adoption," *IEEE Rev. Biomed. Eng.*, vol. 7, pp. 143–153, 2014, doi: 10.1109/RBME.2014.2300234.
[28] A. Demofonti, G. Carpino, L. Zollo, and M. J. Johnson, "Affordable robotics for upper limb stroke rehabilitation in developing countries: A systematic review," *IEEE Trans. Med. Robot. Bionics*, vol. 3, no. 1, pp. 11–20, Feb. 2021, doi: 10.1109/TMRB.2021.3054462.
[29] M. J. Johnson, R. Rai, S. Barathi, R. Mendonca, and K. Bustamante-Valles, "Affordable stroke therapy in high-, low- and middle-income countries: From Theradrive to Rehab CARES, a compact robot gym," *J. Rehabil. Assistive Technol. Eng.*, vol. 4, Jan. 2017, Art. no. 2055668317708732, doi: 10.1177/2055668317708732.
[30] A. J. Veale and S. Q. Xie, "Towards compliant and wearable robotic orthoses: A review of current and emerging actuator technologies," *Med. Eng. Phys.*, vol. 38, no. 4, pp. 317–325, Apr. 2016, doi: 10.1016/j.medengphy.2016.01.010.
[31] Q. Liu, J. Zuo, C. Zhu, and S. Q. Xie, "Design and control of soft rehabilitation robots actuated by pneumatic muscles: State of the art," *Future Gener. Comput. Syst.*, vol. 113, pp. 620–634, Dec. 2020, doi: 10.1016/j.future.2020.06.046.
[32] S. Balasubramanian, R. Wei, M. Perez, B. Shepard, E. Koeneman, J. Koeneman, and J. He, "RUPERT: An exoskeleton robot for assisting rehabilitation of arm functions," in *Proc. Virtual Rehabil.*, Aug. 2008, pp. 163–167, doi: 10.1109/ICVR.2008.4625154.
[33] Q. Liu, A. Liu, W. Meng, Q. Ai, and S. Q. Xie, "Hierarchical compliance control of a soft ankle rehabilitation robot actuated by pneumatic muscles," *Frontiers Neurorobot.*, vol. 11, p. 64, Dec. 2017, doi: 10.3389/fnbot.2017.00064.
[34] W. Zhao and A. Song, "Active motion control of a knee exoskeleton driven by antagonistic pneumatic muscle actuators," *Actuators*, vol. 9, no. 4, p. 134, Dec. 2020, doi: 10.3390/act9040134.
[35] C.-T. Chen, W.-Y. Lien, C.-T. Chen, and Y.-C. Wu, "Implementation of an upper-limb exoskeleton robot driven by pneumatic muscle actuators for rehabilitation," *Actuators*, vol. 9, no. 4, p. 106, Oct. 2020, doi: 10.3390/act9040106.
[36] H. P. Huy Anh, N. N. Son, and C. Van Kien, "Adaptive neural compliant force-position control of serial PAM robot," *J. Intell. Robotic Syst.*, vol. 89, nos. 3–4, pp. 351–369, Mar. 2018, doi: 10.1007/s10846-017-0570-1.
[37] T.-C. Tsai and M.-H. Chiang, "Design and control of a 1-DOF robotic lower-limb system driven by novel single pneumatic artificial muscle," *Appl. Sci.*, vol. 10, no. 1, p. 43, Dec. 2019, doi: 10.3390/app10010043.
[38] C. V. Baysal, "An inverse dynamics-based control approach for compliant control of pneumatic artificial muscles," *Actuators*, vol. 11, no. 4, p. 111, Apr. 2022, doi: 10.3390/act11040111.
[39] S. D. Gasperina, V. Longatelli, F. Braghin, A. Pedrocchi, and M. Gandolla, "Development and electromyographic validation of a compliant human-robot interaction controller for cooperative and personalized neurorehabilitation," *Frontiers Neurorobotics*, vol. 15, Jan. 2022, Art. no. 734130, doi: 10.3389/fnbot.2021.734130.
[40] J. Park, H. Park, and J. Kim, "Performance estimation of the lower limb exoskeleton for plantar flexion using surface electromyography (sEMG) signals," *JBSE*, vol. 12, no. 2, p. 16-595, 2017, doi: 10.1299/jbse.16-00595.
[41] A. Majidirad, Y. Yihun, and L. Cure, "Toward an integrated intervention and assessment of robot-based rehabilitation," *J. Eng. Sci. Med. Diag. Therapy*, vol. 3, no. 2, Mar. 2020, Art. no. 021112, doi: 10.1115/1.4046475.
[42] *Biopac Student Lab Basic System for Win | BSLBSC-W, BSLBSC-M | Education*. BIOPAC Systems, Inc. Accessed: Jul. 9, 2023. [Online]. Available: https://www.biopac.com/product/biopac-student-lab-basic-systems/
[43] D. Farina, W. Jensen, and M. Akay, "Robot-Assisted Neurorehabilitation," Introduction to Neural Engineering for Motor Rehabilitation, IEEE, 2013, pp. 505–528, doi: 10.1002/9781118628522.ch26.



CABBAR V. BAYSAL (Senior Member, IEEE) was born in Adana, Turkey, in 1969. He received the B.S. and M.S. degrees in electrical and electronics engineering from Middle East Technical University, Ankara, Turkey, in 1990 and 1993, respectively, and the Ph.D. degree in electrical and electronics engineering from Cukurova University, Adana, in 2006. From 1993 to 2009, he was an Engineer and the Manager in national and multi-national companies, where he designed and implemented many plant-scale automation projects and electrical power projects. He had also served as a Consultant for industrial projects. From 2009 to 2010, he was with the Robotics Laboratory, UC3M, Spain, as a Visiting Professor. Since 2012, he has been an Assistant Professor with the Department of Biomedical Engineering, Cukurova University. He is the author or coauthor of about 15 research publications between ISI/Scopus papers and conference papers. His current research interests include rehabilitation robotics, bio-inspired robotics, robot hand grasp synthesis, and intelligent control systems.